Westfälische Wilhelms-Universität Münster

Spatially resolved EELS of FeCr layers - an example for processing TEM images with ImageJ

Michael Entrup and Helmut Kohl

Physikalisches Institut und Interdisziplinäres Centrum für Elektronenmikroskopie und Mikroanalyse (ICEM), WWU Münster, Wilhelm-Klemm-Str. 10, 48149 Münster, Germany

http://www.uni-muenster.de/Physik.PI/Kohl/

michael.entrup@uni-muenster.de

MC2013 Regensburg, IM.4.P087

1 Introduction

The measurement of the electron energy loss provides chemical information from a specimen. A transmission electron microscope equipped with an imaging energy filter allows us to create a three-dimensional data cube (Fig. 1). Using energy spectroscopic imaging (ESI) an image with a selected energy interval is acquired (Fig. 1a). In electron energy loss spectroscopy (EELS) from a selected area a single EEL spectrum is acquired (Fig. 1b). When using spatially resolved EELS (SR-EELS) [1], a part of the spatial information is preserved. Several EEL spectra are recorded in parallel as a function of one spatial coordinate, perpendicular to the energy dispersive direction (Fig. 1c). This method is useful for investigating specimens like interfaces and layer systems. We apply SR-EELS in a TEM with an in-column Omega filter to a FeCr layer system. Some of the remaining aberrations of this filter can be corrected by processing the recorded SR-EELS images. We will show how the open source software ImageJ [2] can be used to perform this task.

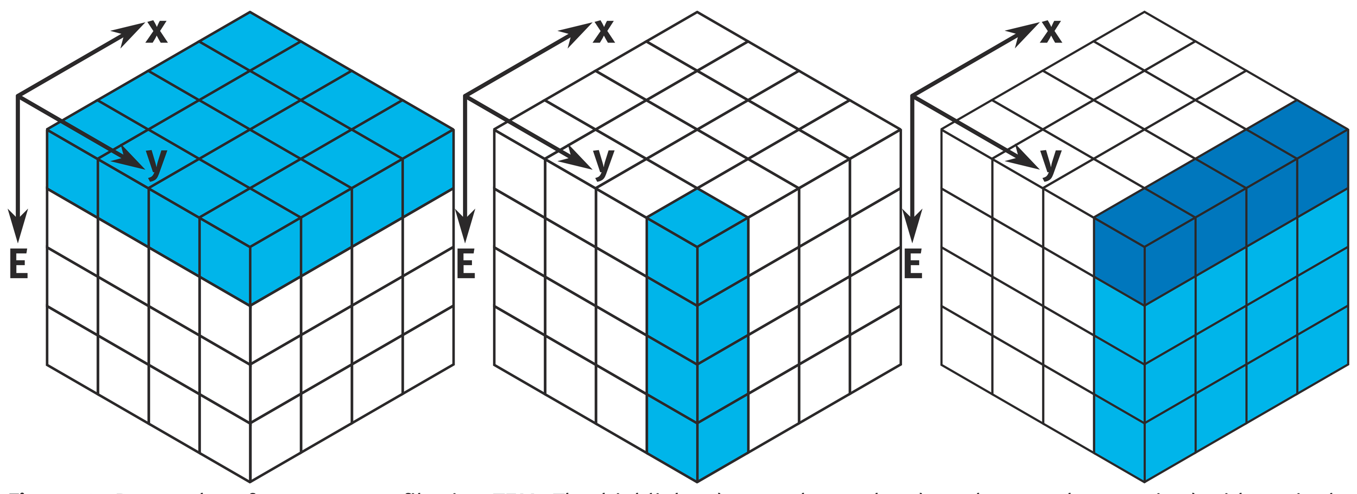

Figure 1: Data cubes for an energy filtering TEM. The highlighted area shows the data that can be acquired with a single measurement by **(a)** electron spectroscopic imaging (ESI), **(b)** EELS and **(c)** SR-EELS.

2 Description of the method

Figure 2 shows a schematic diagram of the corrected Omega filter [3] of a Zeiss Libra 200FE TEM. One-dimensional structures like the alternating layers of Cr and Fe can be analyzed by using SR-EELS. It is necessary to rotate the specimen to orientate the layer boundaries parallel to the energy dispersive direction.

We use binning 8 for the energy dispersive axis and no binning for the perpendicular axis to increase the sensitivity, but still obtain a high spatial resolution. As the spectrum covers only a part of the CCD (about 1/4) it will result in a low spatial resolution when using a binning on this axis. The number of energy channels is reduced from 4096 to 512, which results in a width of 0.16 eV per channel (energy resolution: 0.7 eV).

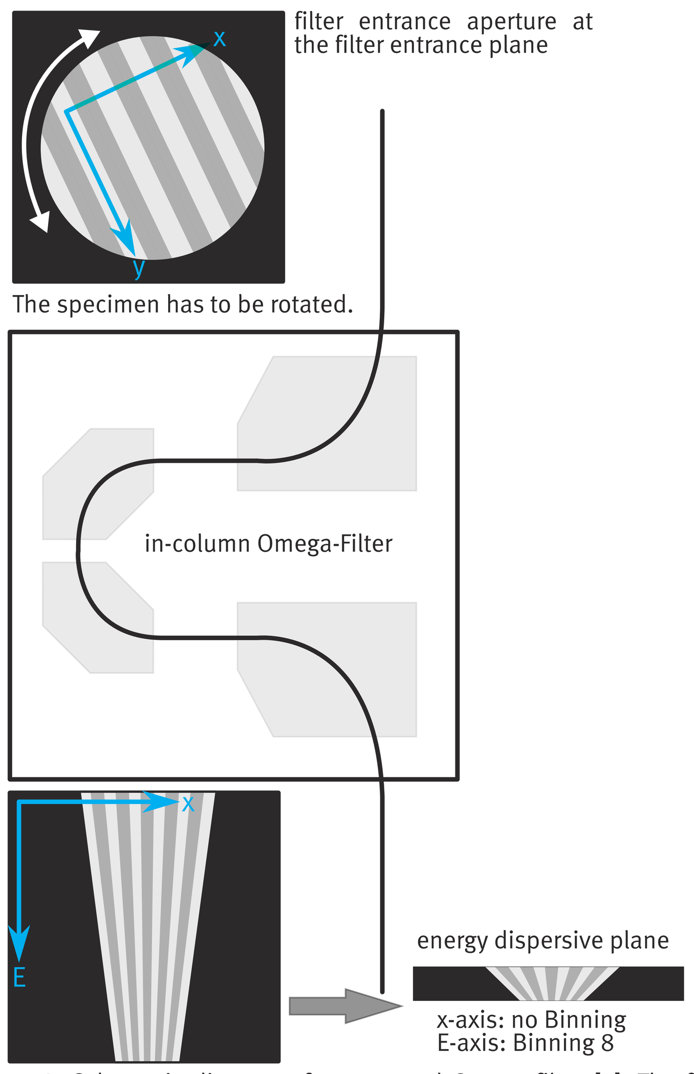

Figure 2: Schematic diagram of a corrected Omega-filter [3]. The filter entrance aperture defines the specimen region that is observed by SR-EELS. To apply SR-EELS it is essential to rotate the specimen.

3

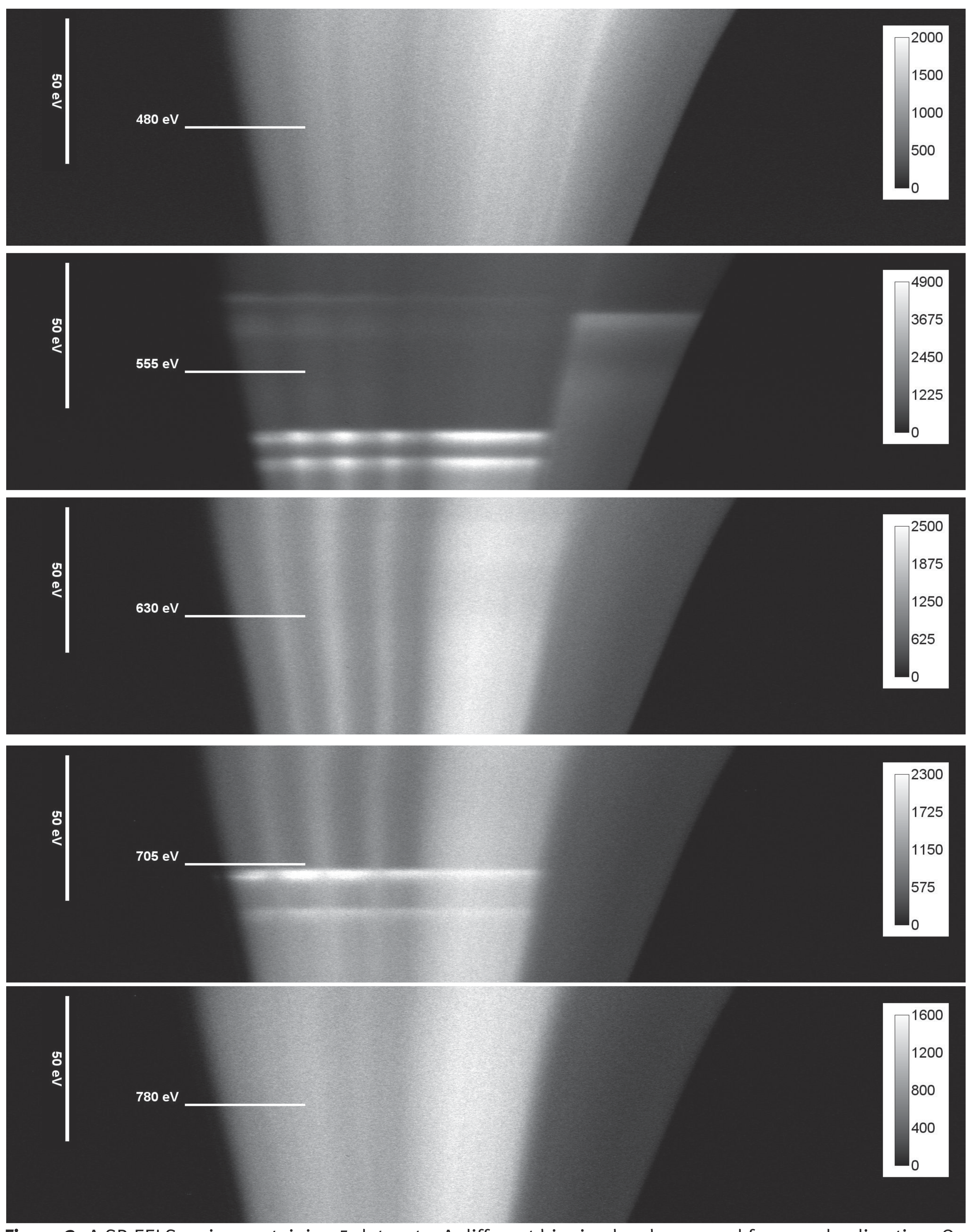

Figure 3: A SR-EELS series containing 5 datasets. A different binning has been used for x- and y-direction. On the x-direction (lateral information) no binning has been used to achieve the highest resolution. On the y-direction (energy loss) binning 8 has been used. The channel width (about 0.16 eV) is still much smaller than the energy resolution of the microscope (Zeiss Libra 200FE with 0.7 eV).

SR_EELS_CorrectionPlugin

The ImageJ plugin (part of EFTEMj [4]) is used to correct the SR-EELS dataset. Each energy channel is scaled to the same lateral size.

Stitching

The ImageJ plugin Stitching [5] is used to splice all 5 corrected SR-EELS datasets.

O- and Cr-Signal

Cornell spectrum imager [6] has been used to subtract the background signal. This is done line by line using a power law model.

Fe-signal

Cornell spectrum imager [6] has been used to subtract the background signal. This is done line by line using a power law model.

4

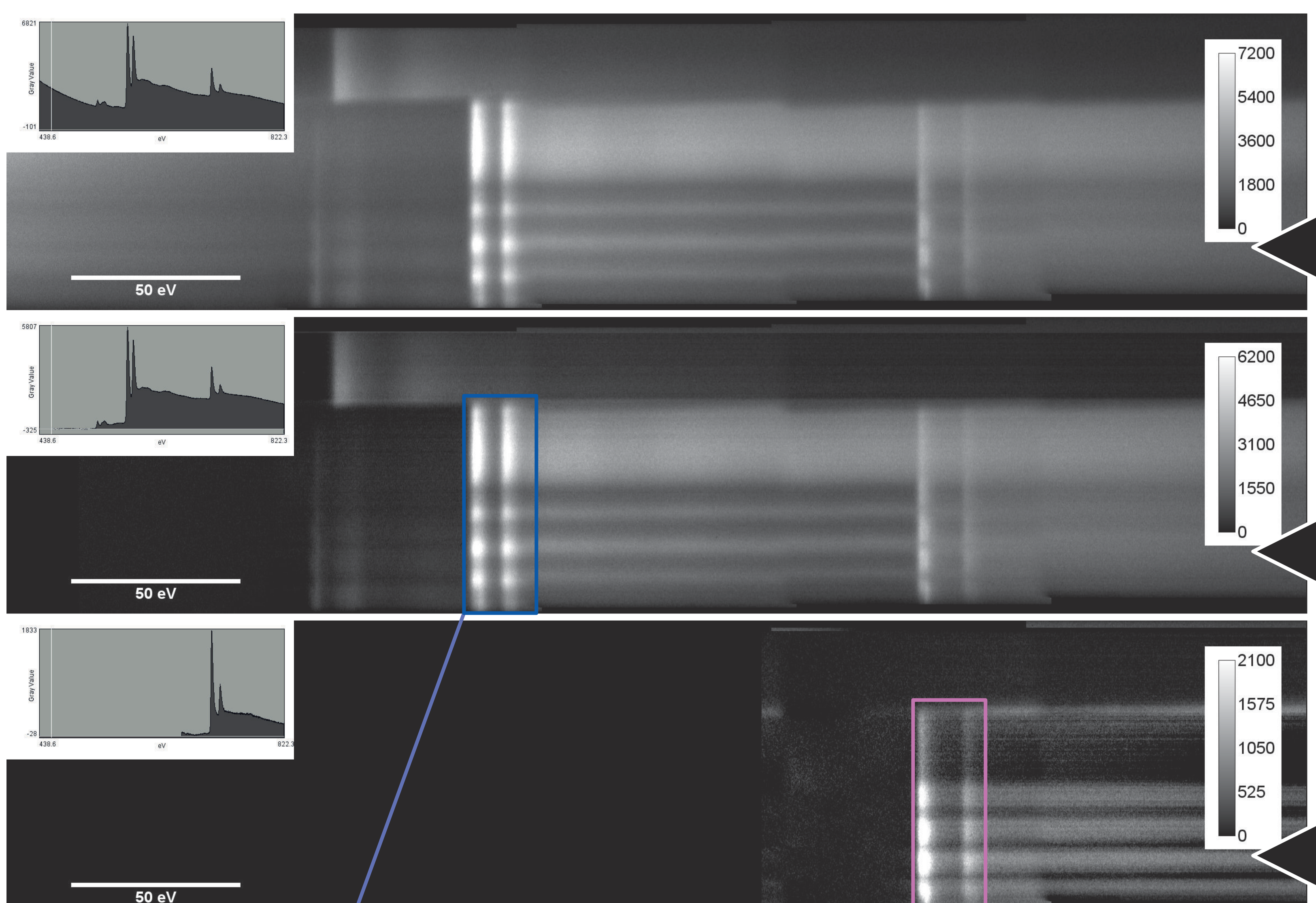

Figure 4: (top) Corrected and stitched SR-EELS series. O-, Cr- and Fe-edges are clearly viable. **(mid)** First background subtraction to extract the O- and Cr-signal. Cornell spectrum imager (CSI) [6] has been used for this task. **(bottom)** Second background subtraction to extract the Fe-signal.

5 Profiles of the integrated elemental signals

Figures 5a and 5b show the integrated elemental signals extracted from the SR-EELS dataset (5a) and from elemental maps created with electron spectroscopic imaging (ESI). The structure looks similar but there is a misalignment at the SR-EELS dataset that distorts the Fe profile and the peak heights (SR-EELS compared to ESI) differ very strongly.

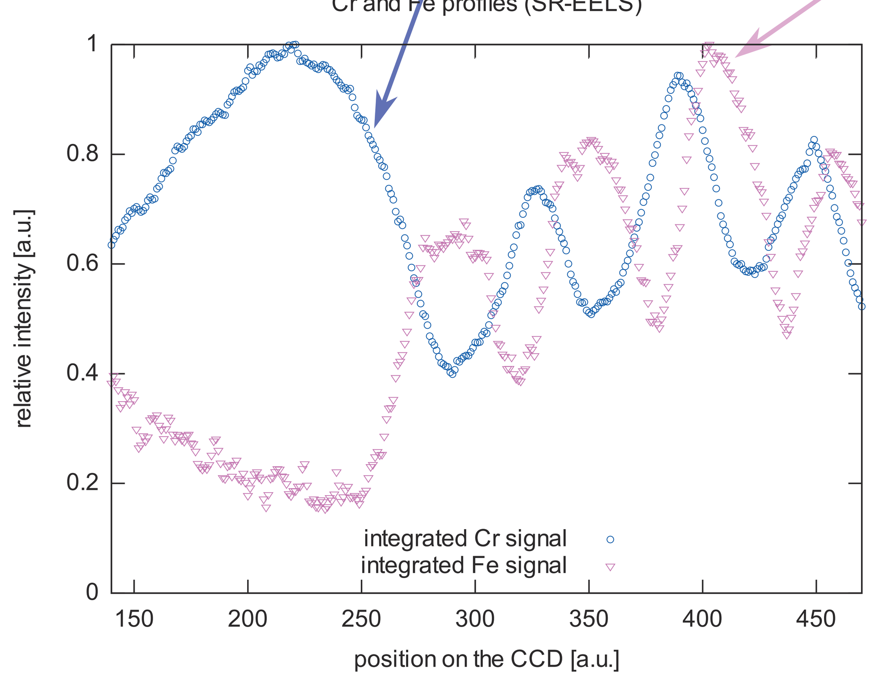

Figure 5a: Integrated signal of Cr an Fe taken from the SR-EELS dataset presented in figure 4. The SR-EELS dataset is not perfectly aligned.

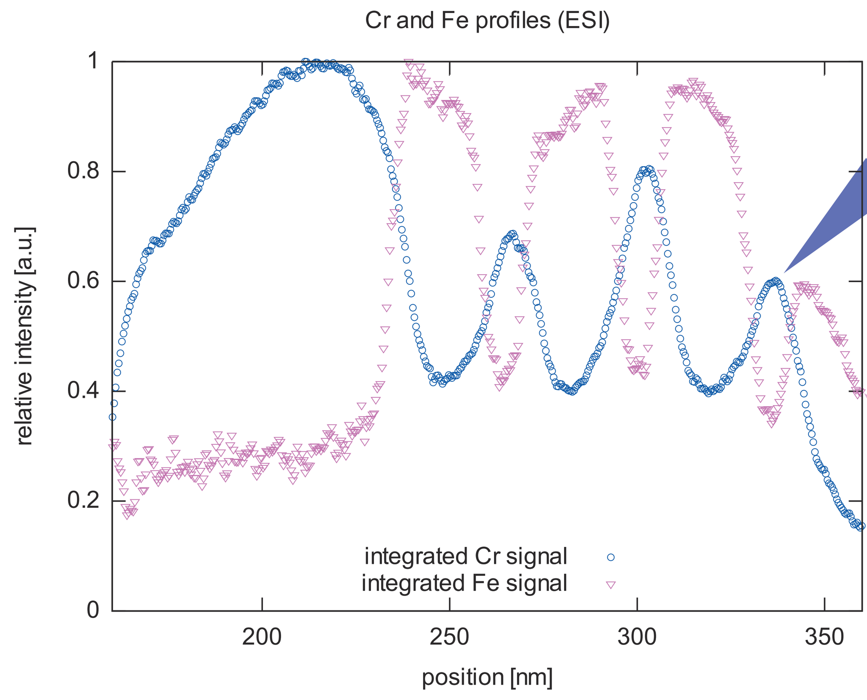

Figure 5b: Integrated signal of Cr an Fe taken from the elemental maps presented in figure 5c.

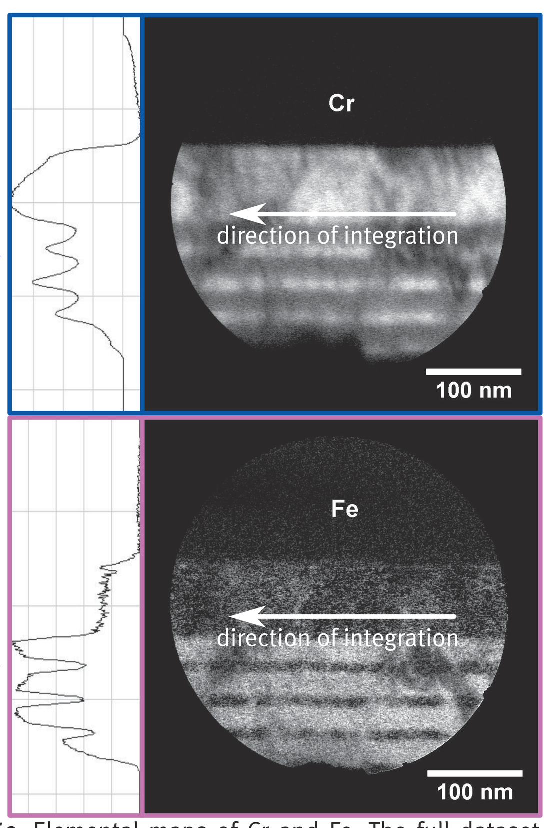

Figure 5c: Elemental maps of Cr and Fe. The full dataset (2x 4 energy filtered images) has been recorded with an acquisition time comparable the the one used to acquire the 5 SR-EELS datasets shown in figure 3.

6 Intensity deviations

Because of the use of a round aperture at the filter entrance plane it is expected that the intensity on the x-axis of a SR-EELS dataset shows a $(1-x^2)^{1/2}$ dependency. Fig. 6 shows a x-axis profile (blue) of a SR-EELS dataset. It is compared to the profile (violet) of a relative thickness map (Fig. 6a) of the same specimen. Large differences are visible at the outer region. A possible reason for this observation is presented in section 7.

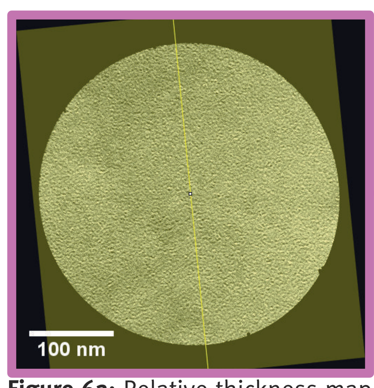

Figure 6a: Relative thickness map of a thin carbon film. The yellow line shows the direction of the plotted profile. Perpendicular to this line an integration is performed.

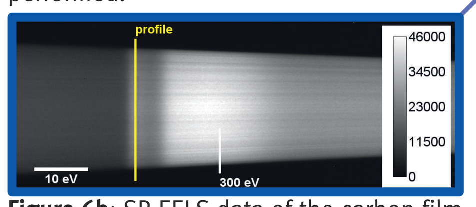

Figure 6b: SR-EELS data of the carbon film section shown in figure 6a.

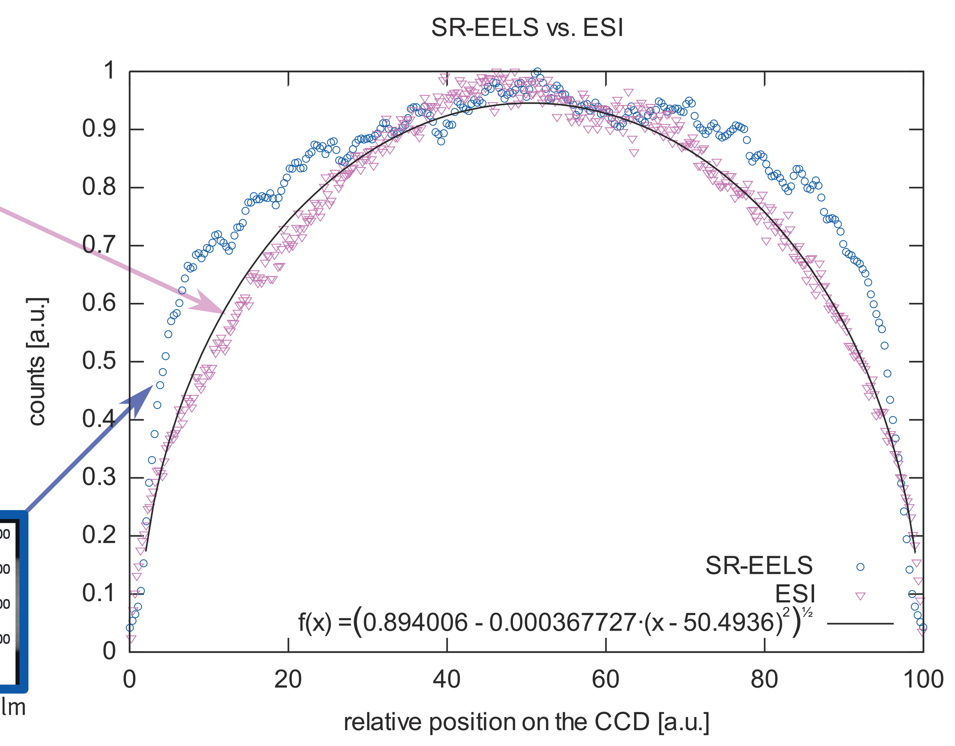

Figure 6: Intensity profiles on an axis perpendicular to the energy dispersive axis.

7 Lateral width of the SR-EELS datasets

The lateral width of the SR-EELS dataset depends on the distance to the optimal ray path. We move the small filter entrance aperture (100 µm) along the axis perpendicular to the energy dispersive axix to probe different distances [7]. It is assumed that the center of the CCD and the optimal ray path are equivalent. This is confirmed by the results of the measurements. With increasing distance to the center the lateral width of the SR-EELS datasets decreases (figure 7). At the edge of the CCD the measured lateral width of the SR-EELS dataset has decreased by 50% compared to the lateral width of the SR-EELS dataset at the center. This change of the lateral dispersion has to be considered when measuring distances at a SR-EELS dataset.

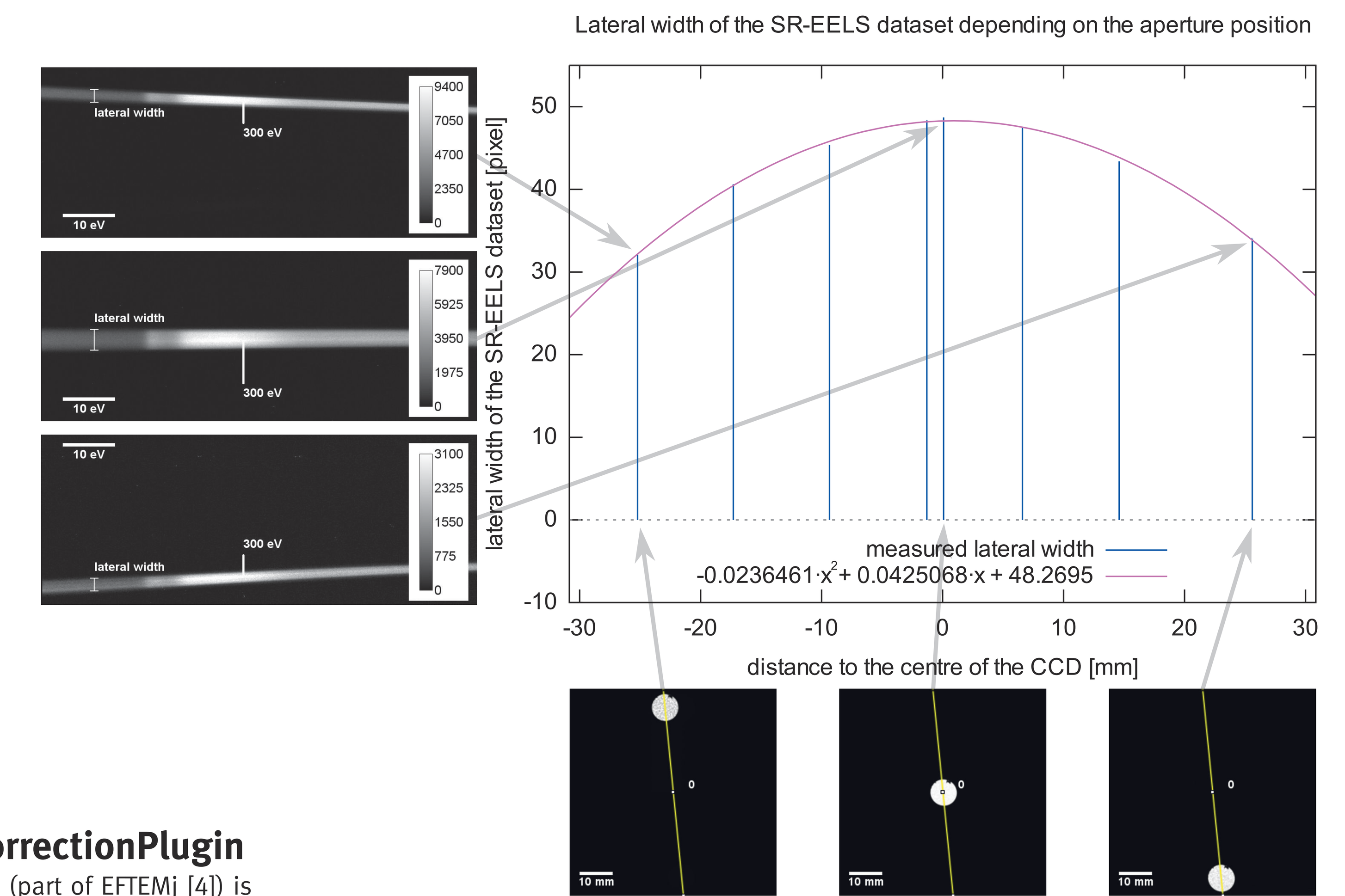

Figure 7: Lateral width of the SR-EELS datasets depending on the position of the filter entrance aperture. The small filter entrance aperture (100 µm instead of 400 µm) has been used for this measurement.

8 Conclusion and Outlook

It is shown that SR-EELS can be used to analyze layer systems. The SR-EELS datasets produced with the in-column Omega filter of the Zeiss Libra 200FE contain two distortions that need to be corrected. The first distortion, the decrease of the spatial extent with increasing energy loss, is corrected by an ImageJ plugin written in Java. The plugin (*SR_EELS_CorrectionPlugin*) has been published as a part of the EFTEMj package [4]. The result of the automatic routine (see figure 4 top) is good but still some optimizations are necessary (see figure 5a). The low signal to noise ratio at the edges of the SR-EELS signal makes it difficult to automatically detect these edges.

The second correction is not yet included into the *SR_EELS_Correction_Plugin*. As figure 7 shows, the lateral width of the SR-EELS datasets depends on the distance to the image center and is exactly described by a parabola. This dependency can easily be corrected along with the intensity variations due to the round aperture at the filter entrance plane. The correction that addresses the varying lateral width is necessary to allow quantitative measurements, for example measuring the layer thickness. The results can be compared to measurements on elemental maps created from ESI series (see figure 5c).

Once the SR-EELS dataset has been corrected, plugins already available for ImageJ can be used for further processing and analysis. Stitching [5] can splice smaller datasets to create a combined dataset of a larger energy loss range. The Cornell spectrum imager (CSI) [6] can be used to subtract the background by using different background models. It will also help to integrate the elemental signal. Finally CSI includes a routine to do principal component analysis (PCA).

Not only plugins for ImageJ can be very useful. The integrated macro language is a powerful tool, too. It is easy to create a macro by using the macro recorder. Even plugins like EFTEMj can be used from within a macro. The use of macros will speed up processing and analysis of a large number of images or datasets. Compared to manual step by step processing a macro will also ensure reproducibility of results.

References:

1. L. Reimer et al. (1988). Operation modes of electron spectroscopic imaging and electron energy-loss spectroscopy in a transmission electron microscope. Ultramicroscopy, **24**, 339-354.
2. C. A. Schneider et al. (2012). NIH Image to ImageJ: 25 years of image analysis. Nature Methods, **9**, 671-675.
3. S. Lanio (1986). Optmierung abbildender Energiefilter für die analytische Elektronenmikroskopie. PhD thesis, TH Darmstadt.
4. https://github.com/EFTEMj/EFTEMj (21.08.2013)
5. S. Preibisch et al. (2009). Globally optimal stitching of tiled 3D microscopic image acquisitions. Bioinformatics, **25**, 1463-1465.
6. P. Cueva et al. (2012). Data Processing for Atomic Resolution Electron Energy Loss Spectroscopy. Microscopy and Microanalysis, **18**, 667-675.
7. R. Hambach and P. Wachsmuth (2012). Momentum-Dispersion in w-q mapping at the SALVE-I. Personal communication, 08.11.2012.
8. The authors gratefully acknowledge funding from the Deutsche Forschungsgemeinschaft (DFG) under grant number Ko885/8-1.

A Appendix - EFTEMj

EFTEMj is a set of plugins for ImageJ. All plugins that are part of EFTEMj are related to energy filtering transmission electron microscopy. The source code is published under an open source license (Simplified BSD License) and can be accessed at GitHub (https://github.com/EFTEMj/EFTEMj or scan the QR-Code on the right). The GitHub repository provides further documentation of the included plugins. For example a process diagram describes the method used with the *SR_EELS_CorrectionPlugin*.

We will give a short overview of the plugins included in EFTEMj:

Previous to the correction of an SR-EELS dataset with *SR_EELS_CorrectionPlugin* the energy loss has to be calibrated. The method used to record the SR-EELS data will not add any meta data to the saved datasets. *SR_EELS_DispersionCalibrationPlugin* will add this meta data by selecting the used acquisition parameters.

Figure 5c shows two elemental maps created from an ESI series. With *ElementalMappingPlugin* EFTEMj offers a plugin that can process an ESI series with an arbitrary number of images to calculate elemental maps. For the background subtraction the power law model is used and the fit is done with a maximum likelihood estimation. More background models and fit methods can easily be added.

When recording an ESI series drift is a problem one has to deal with. EFTEMj includes two plugins that can be used for drift detection and drift correction. Normalized cross-correlation coefficients are used by *DriftDetectionPlugin* to determine the drift between images of an ESI series. By using this method, images with intensities that differ much can be compared easily. The second plugin (*StackShifterPlugin*) compensates the drift by shifting the images.

As EFTEMj is an open source project you are cordially invited to contribute.